

Strong terahertz pulse generation by chirped laser pulses in tenuous gases

W.-M. Wang¹, Z.-M. Sheng^{1,2}, H.-C. Wu³, M. Chen⁴, C. Li¹,
J. Zhang^{1,2}, and K. Mima⁵

¹Beijing National Laboratory of Condensed Matter Physics, Institute of Physics, CAS, Beijing 100190, China

²Department of Physics, Shanghai Jiao Tong University, Shanghai 200240, China

³Max-Planck-Institut für Quantenoptik, D-85748 Garching, Germany

⁴Institut für Theoretische Physik I, Heinrich-Heine-Universität Düsseldorf, D-40225 Düsseldorf, Germany

⁵Institute of Laser Engineering, Osaka University, 2-6 Yamadaoka, Suita, Osaka 565-0871, Japan

zmsheng@sjtu.edu.cn

Abstract: Mechanism of terahertz (THz) pulse generation in gases irradiated by ultrashort laser pulses is investigated theoretically. Quasi-static transverse currents produced by laser field ionization of gases and the longitudinal modulation in formed plasmas are responsible for the THz emission at the electron plasma frequency, as demonstrated by particle-in-cell simulations including field ionization. The THz field amplitude scales linearly with the laser amplitude, which, however, holds only when the latter is at a moderate level. To overcome this limitation, we propose a scheme using chirped laser pulses irradiating on tenuous gas or plasma targets, which can generate THz pulses with amplitude 10-100 times larger than that from the well-known two-color laser scheme, enabling one to obtain THz field up to 10MV/cm with incident laser at $\sim 10^{16}$ W/cm².

© 2008 Optical Society of America

OCIS codes: (300.6270) Spectroscopy, far infrared; (260.5210) Photoionization; (350.5400) Plasmas; (300.2140) Emission;

References and links

1. M. S. Sherwin, C. A. Schmuttenmaer, and P. H. Bucksbaum, *DOE-NSF-NIH Workshop on Opportunities in THz Science* (http://www.er.doe.gov/bes/reports/files/THz_rpt.pdf).
2. B. E. Cole, J. B. Williams, B. T. King, M. S. Sherwin, and C. R. Stanley, "Coherent manipulation of semiconductor quantum bits with terahertz radiation," *Nature (London)* **410**, 60-63 (2001).
3. Z.-M. Sheng, H.-C. Wu, K. Li, and J. Zhang, "Terahertz radiation from the vacuum-plasma interface driven by ultrashort intense laser pulses," *Phys. Rev. E* **69**, 025401(R)/1-4 (2004).
4. Z.-M. Sheng, K. Mima, J. Zhang, and H. Sanuki, "Emission of Electromagnetic Pulses from LaserWakefields through Linear Mode Conversion," *Phys. Rev. Lett.* **94**, 095003/1-4 (2005).
5. W. P. Leemans, C. G. R. Geddes, J. Faure, Cs. Tth, J. van Tilborg, C. B. Schroeder, E. Esarey, G. Fubiani, D. Auerbach, B. Marcellis, M. A. Carnahan, R. A. Kaindl, J. Byrd, and M. C. Martin, "Observation of terahertz emission from a laser-plasma accelerated electron bunch crossing a plasma-vacuum boundary," *Phys. Rev. Lett.* **91**, 074802/1-4 (2003).
6. D. J. Cook and R. M. Hochstrasser, "Intense terahertz pulses by four-wave rectification in air," *Opt. Lett.* **25**, 1210-1212 (2000).

7. M. Kress, T. Löffler, S. Eden, M. Thomson, and H. G. Roskos, "Terahertz-pulse generation by photoionization of air with laser pulses composed of both fundamental and second-harmonic waves," *Opt. Lett.* **29**, 1120-1122 (2004).
8. T. Bartel, P. Gaal, K. Reimann, M. Woerner, and T. Elsaesser, "Generation of single-cycle THz transients with high electric-field amplitudes," *Opt. Lett.* **30**, 2805-2807 (2005).
9. X. Xie, J. Dai, and X.-C. Zhang, "Coherent control of THz wave generation in ambient air," *Phys. Rev. Lett.* **96**, 075005/1-4 (2006).
10. C. D'Amico, A. Houard, M. Franco, B. Prade, A. Mysyrowicz, A. Couairon, and V. T. Tikhonchuk, "Conical Forward THz Emission from Femtosecond-Laser-Beam Filamentation in Air," *Phys. Rev. Lett.* **98**, 235002/1-4 (2007).
11. Y. Liu, A. Houard, B. Prade, S. Akturk, A. Mysyrowicz, and V. T. Tikhonchuk, "Terahertz Radiation Source in Air Based on Bifilamentation of Femtosecond Laser Pulses," *Phys. Rev. Lett.* **99**, 135002/1-4 (2007).
12. H. Hamster, A. Sullivan, S. Gordon, W. White, and R. W. Falcone, "Subpicosecond, electromagnetic pulses from intense laser-plasma interaction," *Phys. Rev. Lett.* **71**, 2725-2728 (1993).
13. K. Y. Kim, J. H. Glowina, A. J. Taylor and G. Rodriguez, "Terahertz emission from ultrafast ionizing air in symmetry-broken laser fields," *Opt. Express* **15**, 4577-4584 (2007).
14. H. C. Wu, J. Meyer-ter-Vehn, and Z. M. Sheng, "Phase-sensitive terahertz emission from gas targets irradiated by few-cycle laser pulses," *New J. Phys.* **10**, 043001/1-10 (2008).
15. M. V. Ammosov, N. B. Delone, and V. P. Krainov, "Tunnel ionization of complex atoms and of atomic ions in an alternating electromagnetic field," *Sov. Phys. JETP* **64**, 1191-1194 (1986).
16. B. M. Penetrante and J. N. Bardsley, "Residual energy in plasmas produced by intense subpicosecond lasers," *Phys. Rev. A* **43**, 3100-3113 (1991).
17. M. Chen, Z.-M. Sheng, J. Zheng, Y.-Y. Ma, and J. Zhang, "Developments and applications of multi-dimensional particle-in-cell codes in the investigation of laser plasma interactions," *Chin. J. Comput. Phys.* **25**, 43-50 (2008).
18. R. Nuter, S. Skupin, and L. Berge, "Chirp-induced dynamics of femtosecond filaments in air," *Opt. Lett.* **30**, 917-919 (2005).
19. G.-Z. Sun, E. Ott, Y. C. Lee, and P. Guzdar, "Self-focusing of short intense pulses in plasmas," *Phys. Fluids* **30**, 526-532 (1987).
20. W.-M. Wang and C.-Y. Zheng, "The evolution of the transverse centroid of asymmetric laser field in plasmas with various density distributions," *Phys. Plasmas* **13**, 053112/1-7 (2006).

1. Introduction

Intense THz pulses with the field strength up to MV/cm or beyond are expected to be important for nonperturbative THz electro-optics, nonlinear THz spectroscopies, THz extreme nonlinear physics in condensed matters, semiconductors, and nanostructured materials, etc. [1, 2], which are mostly unexplored. Such THz pulses are usually obtained from accelerator-based sources, which are still limited by the bandwidth, peak intensity, waveform, as well as the availability to most users. Therefore table-top intense THz sources are attracting significant attention recently. For example, it is found that strong THz radiation can be produced from the laser wakefield in inhomogeneous plasmas by linear mode conversion [3, 4] or from the transition radiation at plasma-vacuum boundaries using ultrashort electron bunches [5]. THz emission can also be produced from tenuous gas targets irradiated with ultrashort laser pulses, which can be realized even using moderately intense laser pulses [6, 7, 8, 9, 10, 11]. Actually Hamster *et al.* observed electromagnetic (EM) emission with the same frequency as the electron plasma frequency ω_p (around the THz frequency for a plasma electron density $n_e = m_e \omega_p^2 / 4\pi e^2 = 1.2 \times 10^{16} \text{cm}^{-3}$) when irradiating helium gas with ultrashort laser pulses in 1993 [12]. In 2000, Cook *et al.* proposed and demonstrated that THz pulses can be generated efficiently when two laser pulses (with one at fundamental and another at the second-harmonic) co-propagate in air [6]. Several authors attributed this THz pulse generation to four-wave rectification [6, 7, 8, 9], and among of them Kress *et al.* found plasma formation is necessary for this THz emission [7]. D'Amico *et al.* proposed the transition-Cherenkov emission from the plasma space charge moving behind the ionization front at light velocity [10, 11]. Recently, Kim *et al.* [13] and Wu *et al.* [14] have suggested that transverse drift currents excited by symmetry-broken laser field ionization of gases are responsible for this THz emission. However, their photocurrent model cannot explain the THz emission frequencies and holds only at moderate laser intensity. Whereas to get

multi-MV/cm THz pulses, one has to invoke strong laser pulses. Under high laser intensity, the ionization can be completed within 1-2 laser cycles and in this case the dependence of THz pulse intensity on laser pulse intensity is still unclear.

In this paper we present an analytical model describing the mechanism of the THz emission in gases irradiated by high intensity lasers and propose a new scheme generating strong THz pulses by use of chirped laser pulses. It is found that the quasi-static transverse drift currents formed during the field ionization process and sequently modulated by formed plasmas in the longitudinal direction are responsible for the THz-wave generation with the frequency ω_p . The THz wave amplitude is proportional to the drift currents dominated by uncontrollable field ionization of gases for either one-color or two-color lasers. Therefore, the THz wave amplitude is not strengthened monotonically with growing laser amplitude for intense lasers. If one takes chirped laser pulses, however, drift currents can be excited efficiently due to the asymmetric field in each laser cycle and the obtained THz wave amplitude can scale linearly with the incident laser amplitude.

2. Theoretical model

Interaction of ultrashort laser pulses with tenuous gases includes laser field ionization of gases and the interaction of the laser pulses with formed plasmas. The laser field ionization rates can be calculated by the ADK formula [15, 16]. For free electrons, they follow the equation of motion given by

$$\partial \mathbf{v}_\perp / \partial t = \partial \mathbf{a}_L / \partial t, \quad (1)$$

where \mathbf{v}_\perp is transverse electron velocity normalized by c , \mathbf{a}_L is laser vector potential normalized by $m_e c^2 / e$. Assume the initial velocity of all newly born free electrons is zero and the j th electron is born at place of x_{j0} and time of t_{j0} . Then the transverse velocity of the electron is $\mathbf{v}_{\perp,j}(x,t) = \mathbf{a}_L(x,t) - \mathbf{a}_L(x_{j0},t_{j0})$ in a plane laser field. The average transverse velocity at x and t is given by

$$\langle \mathbf{v}_\perp \rangle = \sum_{j=1}^N \mathbf{v}_{\perp,j} / N = \mathbf{a}_L - \langle \mathbf{a}_L(x_0, t_0) \rangle, \quad (2)$$

where $\langle \mathbf{a}_L(x_0, t_0) \rangle = \sum_{j=1}^N \mathbf{a}_L(x_{j0}, t_{j0}) / N$, N is the total electron number at x and t , and $\langle \mathbf{a}_L(x_0, t_0) \rangle$ should be a function of $x - ct$. Assume the ionization stops at x_f where laser pulses have left or gas atoms have been ionized completely. Then all $\langle \mathbf{a}_L(x_0, t_0) \rangle$ at $x < x_f$ should be statistically the same and therefore quasi-static transverse currents are formed in the wake of the laser pulses.

When laser pulses just leave x at $t = x/c$, the transverse velocity of all free electrons at x is assumed to be $-\langle \mathbf{a}_L(x_0, t_0) \rangle$. At $t > x/c$, the electron velocity $\mathbf{v}_\perp = \delta \mathbf{a} - \langle \mathbf{a}_L(x_0, t_0) \rangle$, where $\delta \mathbf{a}$ is the vector potential of newly generated EM waves (THz waves). Here we have assumed $\delta \mathbf{a} = 0$ at $t < x/c$ since the newly generated EM wave wavelength is much larger than the laser duration, which will be seen below. Thus, the wave equation of newly generated EM waves in plasmas is given by

$$\left(\frac{\partial^2}{\partial x^2} - \frac{\partial^2}{c^2 \partial t^2} \right) \delta \mathbf{a} = \frac{\omega_p^2}{c^2} [\delta \mathbf{a} - \langle \mathbf{a}_L(x_0, t_0) \rangle], \quad (3)$$

where $\omega_p^2 = 4\pi e^2 n_e / m_e$, the formed plasma electron density n_e is assumed to be uniform since we only consider the case with plasma wavelength $\lambda_p = 2\pi c / \omega_p \gg \lambda_0$ and $|\delta \mathbf{a}| \ll 1$. Solving Eq. (3) by the Laplace transform, one can obtain

$$\begin{aligned} \delta \mathbf{a} = & - \langle \mathbf{a}_L(x_0, t_0) \rangle [\cos(\omega_p \tau) - 1] \\ & + \langle \mathbf{a}_L(x_0, t_0) \rangle [\cos(\omega_p \tau) - 1] \otimes \mathcal{L}^{-1} \left\{ \exp \left[\frac{\xi}{2c} \left(s - \frac{\omega_p^2}{s} \right) \right] \right\}, \end{aligned} \quad (4)$$

where $\xi = ct - x$, $\tau = t$, the convolution operator \otimes is defined by $f(\tau) \otimes g(\tau) = \int_0^\tau f(\tau - t)g(t)dt$, and $\mathcal{L}^{-1}\{F(s)\} = f(\tau)$ is the inverse Laplace transform. The transform $\mathcal{L}^{-1}\{\exp[\frac{\xi}{2c}(s - \frac{\omega_p^2}{s})]\}$ cannot be performed analytically, but it is known that the first term in the exponent represents the propagation effect along the x -direction and the second term means the decaying effect. Equation (4) shows that the THz field $E \propto \partial \delta a / \partial t \propto \omega_p$, i.e., the square root of the plasma density. It also shows that the newly generated EM waves include both ω_p and 0-frequency components and have the same polarization as the incident pulses. When the target has a gas-vacuum boundary, the ω_p -frequency part within about λ_p near the boundary can penetrate into the vacuum effectively.

The above analysis is applicable for gas targets irradiated by either one-color or two-color laser pulses with normalized amplitude $a_L < 1$. When one-color waves are incident, the THz pulses will be produced very inefficiently and have some characteristics of noise. While two-color waves are incident, the symmetry of positive and negative half-cycle of the fundamental wave is broken [13]. The two-color-wave ionization causes drift currents in the same direction in every cycle and thus can emit THz pulses more efficiently than with one-color waves. When the target is a fully ionized plasma slab, either one-color or two-color waves are adopted, the net drift current is null, i.e. $\langle \mathbf{a}_L(x_0, t_0) \rangle = 0$, and no THz pulses can be generated.

3. Simulations

To check the above results, we use one-dimensional (1D) particle-in-cell (PIC) simulations [3, 17]. In our PIC code the field ionization of gases is included with tunnelling ionization rates calculated by the ADK formula [15, 16]. For simplicity, only hydrogen gas (H_2) is used which generates one kind of plasma density only. A slab target with the gas density $n_{gas} = 1.25 \times 10^{-5} n_c$ and the length $L_{gas} = 200\lambda_0$ or $400\lambda_0$ is used starting from $x = 500\lambda_0$, where $n_c = m_e \omega_0^2 / 4\pi e^2$ is the critical density and $\omega_0 = 2\pi/T_0$ is the laser frequency. A laser pulse is incident along the $+x$ direction with the vector potential $\mathbf{a}_L = \hat{\mathbf{e}}_z a_L$, where $a_L = \sin^2(\pi\xi/L_t) \cdot [a_1 \cos(k_0\xi) + a_2 \cos(2k_0\xi + \theta)]$, $k_0 = \omega_0/c$, L_t is pulse duration, a_1 and a_2 are normalized amplitudes for the fundamental and the second-harmonic waves, respectively, and θ is their relative phase. In the following simulations we take $L_t = 20\lambda_0$, $a_2 = a_1/2$, and $\theta = \pi/2$.

Figure 1 is the spatial distribution of transverse currents. In a preformed plasma, no transverse current is left after the laser. However, in a H_2 target a quasi-static negative transverse current is formed. At a later time the current will have a low-frequency oscillating profile [see Fig. 1(c)] because of the plasma modulation. It is indicated that ionization of gases is necessary for the THz emission in this case, which agrees with the above analysis.

The temporal and spacial distribution of THz emission is shown in Fig. 2(a). There are two THz pulses, one going along the $+x$ direction and the other along the $-x$ direction. These THz pulses penetrate into the vacuum and have a waveform with the first cycle strongest, for their current sources within the H_2 plasma decay during radiation. This can be seen more clearly in Fig. 2(b). Figure 2(b) is the temporal evolution of THz pulses observed at $20\lambda_0$ in front of the left gas-vacuum boundary. Their corresponding spectra are plotted by Fig. 2(c). One can see that the THz pulses have frequencies of $0.003\omega_0$ (1THz), $0.005\omega_0$, and $0.01\omega_0$, equal to their individual ω_p . Note that there is the 0-frequency component because of the asymmetry of the positive and negative peaks of the THz pulse. These are consistent with the previous analysis.

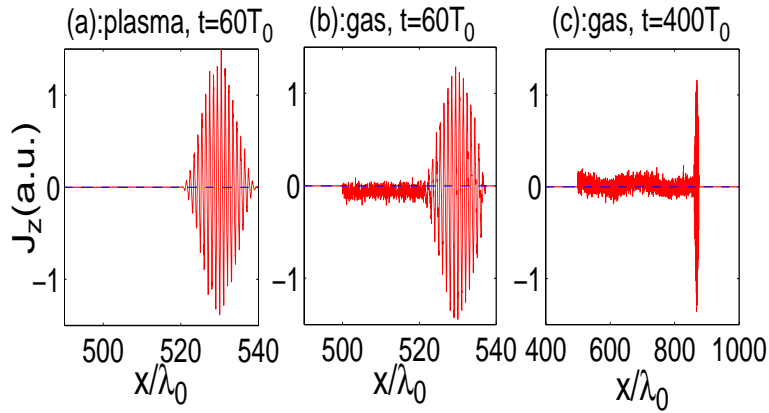


Fig. 1. Spatial distribution of transverse currents in a preformed plasma (a) at $t = 60T_0$ and in a H_2 target at $t = 60T_0$ (b) and $t = 400T_0$ (c), respectively. A two-color laser with $a_1 = 0.06$ and $L_{gas} = 400\lambda_0$ are taken.

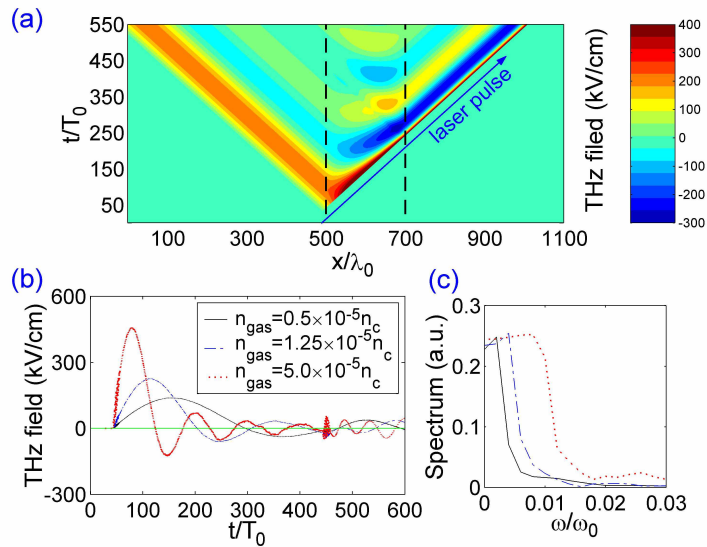


Fig. 2. (a) Temporal and spatial distribution of THz pulses from a H_2 gas target with the density $n_{gas} = 1.25 \times 10^{-5} n_c$. Waveforms (b) and spectra (c) of THz pulses from H_2 targets with different initial gas densities. A two-color laser with $a_1 = 0.06$ is taken.

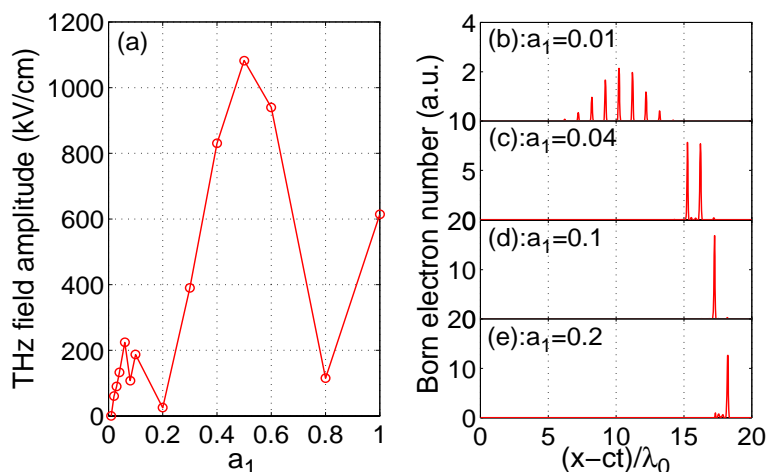


Fig. 3. (a) THz pulse amplitude as a function of a_1 . Frames (b)-(e) show the number of new born electrons produced via laser field ionization against the laser propagation coordinate $x - ct$ for different a_1 and $a_2 = a_1/2$. Two-color lasers and a H_2 target are taken.

For moderately intense incident pulses, experiments in Refs. [6, 7, 8, 9, 13] demonstrated that the THz pulse intensity increases almost linearly with incident pulse intensity. For even intense incident pulses, however, it is not clear whether this still holds. By PIC simulations, we are able to study the THz pulse amplitude as a function of incident laser amplitude within a large range. As shown in Fig. 3(a), at $a_1 \leq 0.06$ the THz pulse amplitude increases with growing a_1 . However, when one increases a_1 further, the THz pulse amplitude does not increase with a_1 monotonically. The reason is that when a_1 is very small, the ionization process lasts for many laser cycles [see Fig. 3(b)] and the produced electron number and the drift current increase with growing a_1 . When a_1 is not small, the ionization process only occurs in the first few cycles and the leading edge of the incident pulse can ionize the gas completely [see Fig. 3(c)]. The peak part of the pulse or the most intense part has no effect on the birth of free electrons or drift current excitation. This can result in the low efficiency in THz emission. When a_1 is increased further, the actual intensity at the part of the pulse ionizing gas may not grow (the part of the pulse ionizing gas is shifted forwards as shown in Figs. 3(d) and (e)). As a result, the drift current or the THz emission may not strengthen with the increasing laser intensity. Therefore, for intense incident pulses it is difficult to control the born places of electrons and produced drift currents, and consequently the THz amplitude does not scale with a_1 monotonically.

It is noted that our above simulations are given with H_2 . When a complex gas such as a rare gas, molecular nitrogen, or air is taken, the features of the THz emission should be qualitatively the same as the H_2 gas. For the same incident laser pulse and gas density, the THz frequency should change due to the different ionization thresholds existing. It is possible that the drift currents produced by field ionization can distribute in a larger region throughout the laser pulse, and the resulting THz pulses have a broader frequency spectrum as compared with the simple H_2 gas.

4. Strong THz emission generation by chirped laser pulses

The unfavorable scaling shown above, which results from the ionization of gases in the two-color scheme, should be overcome in order to achieve high-intensity THz emission. One can adopt another mechanism rather than the field ionization to generate large drift currents which

are the key point producing strong THz emission. Here we propose to use a single chirped laser pulse [18] irradiating on a gas or plasma target, so that electrons can get net acceleration in the transverse direction during each laser period. If fixing the chirping value sign of the laser, the net acceleration of electrons will be found in the same direction in all laser periods, which can cause very strong drift currents. After the laser passes, an electron obtains the transverse drift velocity of $\mathbf{a}_L(L_t) - \mathbf{a}_L(x_{j0}, t_{j0})$ according to Eq. (1), where $\mathbf{a}_L(L_t)$ is the vector potential of the laser pulse at its trailing edge and $\mathbf{a}_L(x_{j0}, t_{j0})$ is relevant with the ionization process. When a large enough chirping value is taken, $|\mathbf{a}_L(L_t)| \gg |\mathbf{a}_L(x_{j0}, t_{j0})|$ for a gas target, which closes to the case in a preformed plasma with $a_L(x_{j0}, t_{j0}) \equiv 0$. For simplicity, we shall only take plasma targets with $\mathbf{a}_L(L_t) - \mathbf{a}_L(x_{j0}, t_{j0}) \equiv \mathbf{a}_L(L_t)$ and Eq. (4) holds with substituting $\mathbf{a}_L(L_t)$ for $-\langle \mathbf{a}_L(x_0, t_0) \rangle$ in this case. Therefore, obtained THz pulse amplitude will be in proportion with $\mathbf{a}_L(L_t)$ or the incident laser amplitude.

In order to demonstrate the scheme mentioned above in a simple way, we take the chirped pulse electric field $\mathbf{E}_L = \hat{\mathbf{e}}_z \varepsilon_L$ normalized by $m_e \omega_0 c / e$, with

$$\varepsilon_L = a_0 \sin[k_0 \xi (1 + C\xi)] \sin(\pi \xi / L_t^C), \quad (5)$$

where the pulse duration $L_t^C = (\sqrt{1 + 4CL_t^0} - 1)/2C$ for the chirping parameter C and L_t^0 is the pulse duration at $C = 0$. For positively-chirped pulses $C > 0$, $L_t^C < L_t^0$ and for negatively-chirped pulses $C < 0$, $L_t^C > L_t^0$, when the total period number of laser pulses stays the same at any given C . Taking such chirped pulses, one can easily calculate the net transverse drift velocity $v_\perp(L_t^C)$ or $a_L(L_t^C)$ through $a_L(L_t^C) = -\int_0^{L_t^C} \varepsilon_L(\xi) d\xi$ for any C . For example, when $C = 1.0$ and -0.024 , there are $a_L(L_t^C) = 0.0115a_0$ and $-0.0413a_0$, respectively. Then obtained THz pulse amplitude $\delta a \propto 0.0115a_0$ and $-0.0413a_0$ for $C = 1.0$ and -0.024 , respectively, according to Eq. (4). To test the validity of this analysis, we conduct PIC simulations with $C = 1.0$ and $C = -0.024$, taking $L_t^0 = 10\lambda_0$. We fix the C or keep the chirped pulse profile and change the pulse amplitude to study the obtained THz pulse amplitude as a function of a_0 , which shown in Fig. 4(a). One see that the THz pulse amplitude increases linearly with a_0 for both positive and negative chirped pulses, which is in good agreement with the previous analysis. Further, the ratio of slopes $[\partial(\delta a)/\partial a_0|_{C=-0.024}]/[\partial(\delta a)/\partial a_0|_{C=1.0}] = -3.59$ is exactly confirmed by the results of Fig. 4(a). Moreover, compared with the scaling shown in Fig. 3(a), the THz pulse amplitude found for the chirped pulse with $C = -0.024$ is as 10-100 times large as that in the two-color scheme for a wide range of the incident laser amplitude. When $a_0 = 0.067$, the THz amplitude is up to $1MV/cm$ at the given plasma density of $2.5 \times 10^{-5}n_c$, corresponding to the frequency of 1.5 THz.

A two-dimensional (2D) PIC simulation is conducted to illustrate the multi-dimensional properties of the THz emission. We take the initial electron density $4 \times 10^{-4}n_c$ (corresponding to the frequency of 6 THz), a chirped laser pulse with $a_0 = 0.1$, the transverse radius of $8\lambda_0$, and $C = -0.024$, as well as the simulation box of $800\lambda_0 \times 80\lambda_0$ (*in x* \times *y*). Figure 4(b) is spacial distribution of THz pulses. One can see there are two THz pulses generated with one propagating along the +x direction and another along the -x direction. They have a transverse profile like that of the incident laser, which accords with our previous results that the THz pulse amplitude is proportional to the laser amplitude. The emission has a wavelength around $\lambda_p = 50\lambda_0$ and it has the highest intensity in the first cycle with amplitude exceeding $7MV/cm$. This amplitude is about 4 times of the one in Fig. 4(a) for the same a_0 , which agrees with Eq. (4) that the THz field is proportional to ω_p . For the convenience of experimentalists, we rewrite here the 2D simulation parameters with common units that the plasma electron density $4.5 \times 10^{17}cm^{-3}$, the laser wavelength $800nm$, the peak intensity $2.1 \times 10^{16}W/cm^2$, the transverse radius $6.4\mu m$, the duration $44fs$, and the chirped parameter $C = -0.024$.

It should be pointed that our 1D and 2D PIC simulation results presented previously have not

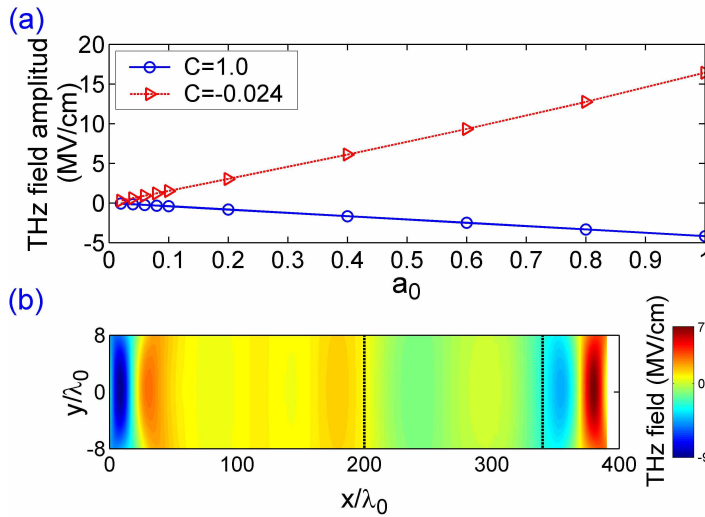


Fig. 4. (a) THz pulse amplitude as a function of the chirped laser amplitude for two different chirping parameters, where the electron density is $2.5 \times 10^{-5} n_c$; (b) Spatial distribution of THz pulses simulated by 2D PIC, where the electron density is $4 \times 10^{-4} n_c$ and a chirped laser pulse with $a_0 = 0.1$, the transverse radius of $8\lambda_0$, and $C = -0.024$ is used. Plasma targets are taken.

completely considered propagation effects of light, especially for large distance propagation. In three-dimensional cases, the produced THz pulse and the laser pulse can evolve completely. The laser pulse may experience self-focusing provided the critical power P_{cr} [19, 20] is exceeded, while the THz pulse may spread very quickly due to small spot size comparable to the THz wavelength. As a result, the linear scaling of the THz emission amplitude with the initial incident laser amplitude could be deviated.

5. Conclusion

In conclusion, we have studied the mechanism of THz pulse generation from gas targets irradiated by ultrashort intense laser pulses. The quasi-static transverse currents created by laser field ionization and sequent modulation in formed plasmas are responsible for the THz emission. In the well-studied two-color laser scheme, it is found that the THz pulse amplitude scales linearly with the incident laser amplitude only when the latter is moderately large. This presents a significant limitation for the generation high power THz emission over the field strength of MV/cm , necessary for high field THz physics. To overcome this, we propose to use chirped laser pulses, with which even strong THz pulses can be generated with amplitudes scaling linearly with the laser amplitude.

Acknowledgments

This work was supported in part by the National Natural Science Foundation of China (Grants No. 10425416, 10674175, 60621063), the National High-Tech ICF Committee in China, the National Basic Research Program of China (Grant No. 2007CB815105) and the JSPS-CAS Core-University Program on Plasma and Nuclear Fusion.